American Journal of Pathology, Vol. 167, No. 5, November 2005

Tumorigenesis and Neoplastic Progression

Rapid Vessel Regression, Protease Inhibition, and Stromal Normalization upon Short-Term Vascular Endothelial Growth Factor Receptor 2 Inhibition in Skin Carcinoma Heterotransplants

Daniel W. Miller,*† Silvia Vosseler,* Nicolae Mirancea,* Daniel J. Hicklin,‡ Peter Bohlen,‡ Hans E. Völcker,† Frank G. Holz,†§ and Norbert E. Fusenig*

From the Division of Differentiation and Carcinogenesis, German Cancer Research Center, Heidelberg, Germany; the Department of Ophthalmology,† University of Heidelberg Hospitals and Clinics, Heidelberg, Germany; the Department of Ophthalmology,§ University of Bonn, Bonn, Germany; and ImClone Systems Incorporated,‡ New York, New York*

Vascular endothelial growth factor (VEGF) plays a key role in tumor angiogenesis, and blockade of VEGF receptor 2 (VEGFR-2), with the monoclonal antibody DC101, inhibits angiogenesis and tumor growth. To examine the short-term effects of DC101, we surface transplanted the squamous cell carcinoma cell line A5-RT3 onto nude mice. After short-term treatment with DC101, we observed rapid reduction in vascularization and reversion of the tumor phenotype. Beginning 24 hours after treatment, VEGFR-2 inhibition resulted in decreased vessel density within the tenascin-c-staining tumor-associated stroma and reduced endothelial cell proliferation. Stromal expression of matrix metalloproteinase-9 and -13 was drastically reduced 96 hours after VEGFR-2 inhibition as detected by *in situ* hybridization and *in situ* zymography. Moreover, the morphology of the tumor-stroma border changed from a highly invasive carcinoma to a well-demarcated, premalignant phenotype. The latter was characterized by the appearance of a regular basement membrane in immunostaining and ultrastructural analyses. These findings suggest that VEGFR-2 inhibition by DC101 evokes very rapid reduction of preformed vessels and decreases both stromal protease expression and gelatinolytic activity, resulting in the modulation of the tumor-stroma border zone and reversion of the tumor phenotype. Thus, short-term inhibition of VEGF signaling results in complex stromal alterations with crucial consequences for the tumor phenotype. *(Am J Pathol 2005, 167:1389–1403)*

The formation of new vessels from pre-existing ones, termed angiogenesis, occurs physiologically in the reproductive cycle, wound healing, and ocular maturation as well as in a number of pathologies including cancer, age-related macular degeneration, and diabetic retinopathy.[1,2] Better understanding of angiogenesis and its mechanisms will optimize current therapies directed at treating these diseases and will provide new therapeutic targets directed against them.[3,4] The work described here analyzed the immediate effects of inhibition of vascular endothelial growth factor (VEGF) signaling on vascular regression and normalization of the tumor-stromal interface.

The study of new vessel formation is dependent on the existence of adequate model systems for angiogenic related diseases. Current *in vitro* cancer models are only partially capable of mimicking the complex interaction between tumor cells, vasculature, and stromal elements that occur *in vivo.*[5] To better understand the complex interplay between these compartments, we have previously developed an *in vivo* assay of tumor invasion with the aid of matrix-inserted surface transplants.[5] This assay involves the growth of a cell monolayer on a collagen gel, which is grafted within a silicon chamber onto the back muscle fascia of a nude mouse, resulting in the growth of a stratified epithelium that allows for the study of tumor-stromal interactions, including angiogenesis, at different

Supported by the European Union (grant QLK-CT-2002-02136) and the Deutsche Forschungsgemeinschaft (grant Ho 1926/2-1).

D.W.M. and S.V. contributed equally to this work.

Accepted for publication July 19, 2005.

Address reprint requests to Norbert E. Fusenig, Division of Differentiation and Carcinogenesis (A080), German Cancer Research Center (DKFZ) INF 280, 69120 Heidelberg, Germany. E-mail: n.fusenig@dkfz.de.

stages in a polarized manner.[5–7] Although initially separated by the interposed collagen gel, transplanted cells rapidly stimulate the formation of granulation tissue, including vascular sprouting, from the host side. On replacement of the interposed collagen matrix by the newly formed granulation tissue, tumor invasion commences in malignant transplants, whereas normal and benign cells remain as an intact stratified surface epithelia inducing only transient angiogenesis.[6,8] Furthermore, we have successfully used this assay to selectively manipulate numerous components of the tumor-stromal system for the better understanding of their role in angiogenesis and tumor growth.[8–16]

Among other components, we have also studied the role of VEGF in this system. VEGF is considered to be a key regulatory molecule in angiogenesis in which it induces vascular growth and permeability while acting as a survival factor for newly formed vessels.[17] One of its receptors, VEGFR-2 is the major mediator of VEGF's mitogenic and permeability enhancing effects in endothelial cells.[3,18] By blocking signaling of VEGFR-2 with the antibody DC101,[19] we have demonstrated inhibition of tumor vascularization and abrogation of tumor invasion using this assay.[8] Systemic and chronic administration of DC101 to animals carrying surface transplants of the highly aggressive and metastasizing human squamous cell carcinoma cell line A-5RT3 resulted in reversion of the tumor phenotype with a normalized tumor-stroma border including a well-demarcated basement membrane.[20,21] These initial experiments examined long-term effects of multiple DC101 treatments on tumor phenotype and raised numerous questions about which mechanisms were responsible for the effects of VEGFR-2 inhibition on tumor-stromal interactions.

An important question was whether DC101-induced changes in the tumor stroma were due to chronic treatment or if they could be observed as immediate effects of limited treatments, whose mechanisms of action could be studied. The study described here examined the early effects of VEGFR-2 inhibition on tumor phenotype by using the surface transplant model described above. Beginning 3 hours after systemic administration of the VEGFR-2 blocking antibody DC101, vascular density, endothelial proliferation, protease expression, and tumor-stromal interactions were analyzed until 96 hours after initial DC101 treatment for the response to VEGFR-2 inhibition.

Materials and Methods

Cells and Culture Conditions

The highly malignant tumorigenic clone (A-5RT3) was derived from the immortalized human keratinocyte cell line HaCaT[10] after transfection with the c-Ha-ras oncogene and recultivation of heterotransplants in nude mice, as described previously.[7,11,20] All cells were grown in enriched minimum essential medium (4×) supplemented with 5% fetal calf serum and 200 μg/ml geneticin as described previously.[20]

Surface Transplantation Assay

Cells were transplanted onto the dorsal muscle fascia of 7- to 9-week-old nude mice (Swiss/c nu/nu back crosses) as monolayer cultures growing on collagen type 1 gels using a silicone chamber device, as described in detail.[5,8] Transplants were dissected *en bloc*, embedded in Tissue-Tek (Miles Laboratories, Elkhart, IN), and frozen in liquid nitrogen vapor for preparation of cryostat sections. For labeling of proliferating cells, mice received tail vein injections of 5-bromodeoxyuridine (BrdU) and 2-deoxycytidine (65 mmol/L each) in 0.9% NaCl (100 μl) 1.5 hours before being sacrificed.

VEGFR-2 Inhibition by DC101

The *in vivo* anti-angiogenic activity of the VEGFR-2 neutralizing antibody DC101 was tested in mice carrying transplants of the highly malignant keratinocyte clone HaCaT-ras A-5RT3 starting 18 days after transplantation,[20] when invasive tumor tissues had formed.[20] Mice received intraperitoneal injections of the monoclonal antibody DC101 [800 μg per mouse in 150 μl of phosphate-buffered saline (PBS)] or PBS alone at 0 hours and 48 hours after initial injection. Transplants were dissected at 3, 6, 24, 48, 72, and 96 hours after initial injection with all animals after the 48-hour time point receiving a second DC101 injection at 48 hours. The experiment was performed with three animals per time point and repeated two times. All animal experiments were performed in compliance with the relevant laws and institutional guidelines with permission of the Regierungspräsidium Karlsruhe, dated 7.4.1999 and 11.3.2003 (AZ 35-9185.81/G-16/03).

Antibodies and cDNAs

The rat monoclonal antibody DC101 to mouse VEGFR-2 (flk-1) was obtained from ImClone Systems Inc. (New York, NY) and described in detail previously.[19] Rat monoclonal antibody against mouse CD31 was obtained from BD PharMingen (Heidelberg, Germany), guinea pig polyclonal pan-keratin anti-serum from Progen (Heidelberg, Germany), sheep polyclonal antibody against BrdU from NatuTec (Frankfurt, Germany), rabbit polyclonal antibody against tenascin-c from Telios Pharmaceuticals (San Diego, CA), rabbit polyclonal antibody against mouse collagen type IV was from Novotec (Lyon, France), rat monoclonal antibody against mouse neutrophil granulocytes from Serotec (Düsseldorf, Germany), and sheep polyclonal antibody against mouse matrix metalloproteinase (MMP)-9 was a gift from Prof. Gillian Murphy (University of Cambridge, Cambridge, UK). Secondary antibodies were obtained from Dianova (Hamburg, Germany) and Hoechst 33258 bisbenzimide for nuclear staining from Sigma-Aldrich (Taufkirchen, Germany). Mouse cDNA encoding MMP-9 was from Novus Molecular Inc. (San Di-

ego, CA) and mouse MMP-13 cDNA was a gift from Dr. Peter Angel (Deutsches Krebsforschungszentrum, Heidelberg, Germany).

Indirect Immunofluorescence

For immunofluorescence staining, frozen sections were fixed for 5 minutes in 80% methanol at 4°C and 2 minutes in acetone at −20°C, and rehydrated in PBS. For BrdU localization in DNA, sections were additionally denatured in 2 mol/L HCl for 10 minutes at room temperature and washed (3 × 10 minutes). Primary antibodies were incubated in 12% bovine serum albumin/PBS at room temperature for 2 hours or 4°C overnight. After washing (3 × 10 minutes) sections were incubated with appropriate secondary antibodies together with 5 μg/ml Hoechst bisbenzimide for staining of cell nuclei. Before embedding in Permafluor (Immunotech, Marseille, France) sections were washed again (3 × 10 minutes) in PBS. Detection of apoptotic cells was performed using the In Situ Cell Death Detection kit (Roche, Mannheim, Germany) following the manufacturer's protocol. Stained sections were examined and photographed with an Olympus AX-70 microscope (Olympus, Hamburg, Germany) fitted with epifluorescence optics and connected to a PC using Analysis Imaging Software (Soft Imaging Systems GmbH, Münster, Germany).

Quantification of Vascular Regression and Endothelial Proliferation

Quantification of Microvessel Density in Stromal Strands

The heterotransplant assay used here, involves the growth of a tumor cell monolayer on a collagen gel, which is grafted within a silicon chamber onto a nude mouse. In this model system, stratified tumor epithelium forms from the cell monolayer. This, in turn, induces murine stroma formation from the host toward the stratified cell layer. Subsequently, tumor cells then invade the stroma allowing for the analysis of tumor-stromal interactions in a polarized manner.[5–7] Areas of stromal infiltration into the tumor, the leading edge of vascular growth thought to contain the most immature vessels, were chosen for quantification. In immunostaining, the extracellular matrix (ECM) of these areas was strongly stained by antibodies to tenascin-c, a major component of the tumor stroma,[22] whereas associated vessels were strongly stained by antibodies against CD31. Photos were taken over the entire area to the edge of the stromal and tumor cell fronts from sections of two to four animals depending on the time points quantified (control 24 hours, three animals; control 48 hours; two animals; DC101 treated 3 hours, two animals; DC101 treated 24 hours, four animals; DC101 treated 48 hours, three animals; DC101 treated 72 hours, two animals; DC101 96 hours, two animals). The area of tenascin-c and CD31 staining per photograph was quantified using Analysis Imaging Software. The CD31 staining area was then divided by the tenascin-c area of each photograph to obtain a percent value. Means and standard deviations were calculated using Microsoft Excel for each time point measured. A nonpaired Mann-Whitney test was performed between controls and treated time points using SAS Stat View (SAS, Heidelberg, Germany). All column diagrams were made using Microsoft Excel (Microsoft Deutschland GmbH, Unterschleissheim, Germany).

BrdU Quantification

Serial sections from the same animals analyzed for tenascin-c and CD31 quantification were stained for BrdU, Hoechst, and collagen IV using the immunofluorescence techniques described above. Stromal areas were photographed as described above and endothelial nuclei (those located within collagen IV staining luminal areas) staining for Hoechst and those for BrdU were counted. A percentage of those nuclei staining positive for both BrdU and Hoechst was made, with means and standard deviations being calculated with Microsoft Excel. A nonpaired Mann-Whitney test was performed between controls and treated time points using SAS Stat View. All column diagrams were also made using Microsoft Excel.

In Situ *Hybridization*

In situ hybridization was performed as described.[8,21] In brief, Digoxenin (DIG)-labeled RNA probes for mouse MMP-9 and MMP-13 were prepared using T7, SP6, or T3 RNA polymerase (for anti-sense and sense, respectively) according to the manufacturer's instructions (Roche, Mannheim, Germany). Cryostat sections were fixed in 4% paraformaldehyde, pretreated, hybridized, and washed at high stringency as described.[23] DIG was labeled by anti-DIG-AP (Roche) and alkaline-phosphatase reaction was detected by NBT/BCIP (Gibco-Life Technologies/Invitrogen, Eggenstein-Leopoldshafen, Germany). After DIG *in situ* hybridization of MMP-9 or MMP-13 counterstaining was performed by indirect immunofluorescence with antisera against pankeratin and collagen type IV. Sections were photographed with different channels being assigned different colors for further analysis using Analysis Imaging Software.

In Situ *Zymography*

Gelatinolytic activity was demonstrated in unfixed cryostat sections using DQ gelatin (EnzChek; Molecular Probes, Leiden, The Netherlands) as a substrate. Cryostat sections (7 μm) were incubated with 40 μg/ml DQ gelatin for 30 minutes at room temperature. After washing (3 × 10 minutes) sections were stained for CD31 and Hoechst using immunofluorescence techniques described above.

Quantification of Gelatinolytic Activity

Areas of gelatinolytic activity staining were quantified in vision fields (0.38 mm^2) from sections of two to four

animals per time point stained with DQ gelatin using Analysis Imaging Software.

Transmission Electron Microscopy

Fresh samples of A-5RT3 transplants of control and DC101-treated mice (two animals per time point) were prefixed in ice-cold 4% glutaraldehyde in 0.2 mol/L sodium cacodylate buffer, pH 7.3, for 3 hours and postfixed in 2% osmium tetroxide in 0.1 mol/L sodium cacodylate buffer for 2.5 hours at 4°C. Tissue blocs were then washed with distilled H_2O, stained *en bloc* with 0.5% aqueous uranyl acetate overnight at 4°C, and again washed with distilled H_2O. After dehydration through two graded series of ethanol and infiltration with propylene oxide, specimens were embedded in Epon 812-equivalent (glycidether 100; Serva, Heidelberg, Germany) and finally polymerized at 60°C for 48 hours. Semithin sections of 1 μm were stained with 0.1% toluidine blue for light microscopy. Ultrathin sections (50 to 90 nm) were cut by a Reichert Young ultramicrotome (Leica Microsystems Nussloch GmbH, Nussloch, Germany), counterstained with uranyl acetate, and subsequently lead citrate, and examined with a Zeiss EM10B electron microscope (Carl Zeiss NTS GmbH, Oberkochen, Germany). Samples were cut from the top of the surface transplant containing tumor epithelium toward the underlying stroma to accurately analyze the tumor-stromal border.

Results

Inhibition of Tumor Vascularization and Invasion through VEGFR-2 Inhibition

As shown recently, long-term application of the monoclonal antibody DC101 blocks angiogenesis, normalizes the tumor-stroma border zone, and reverts tumor phenotype.[21] To better visualize and understand the altered interactions between tumor and stromal cells, early time points after inhibition of angiogenesis were analyzed using the same A-5RT3 carcinoma cells in surface transplants.[5,8] This assay involves the growth of a tumor cell monolayer on a collagen gel, which is grafted within a silicon chamber onto a nude mouse. In this model system, stratified tumor epithelium forms from the cell monolayer. This, in turn, induces murine stroma formation from the host toward the stratified cell layer. Subsequently, tumor cells then invade the stroma allowing for the analysis of tumor-stromal interactions in a polarized manner (Figure 1A).[5–7] The A-5RT3 tumor cell transplants studied here, induced rapid stromal activation with accumulation of fibroblasts and inflammatory cells and growth of new blood vessels in a directed and well-defined pattern. This was followed by tumor cell invasion and reciprocal infiltration of vascularized stromal strands into the tumor parenchyma, as visualized by differential immunostaining of tumor cells, with antibodies to keratin, and endothelial cells, with antibodies to CD31, at 24 days after transplantation in control animals (Figure 1B).

Beginning 24 hours and progressively continuing through 96 hours of DC101 treatment, vascularization of the tumor tissue was rapidly reversed and tumor invasion was strongly inhibited (Figure 1, C and D, compared to B). In particular, stromal areas localized within the tumor parenchyma showed reduced numbers of CD31 staining vessels at 72 and 96 hours after DC101 treatment (Figure 1, C and D; arrowheads). This suggested that VEGFR-2 inhibition not only limited the formation of new vessels but may have also caused rapid regression of pre-existing vessels. Moreover, the avascular but vital tumor tissue exhibited only minor invasion into the underlying stromal tissue. As a consequence of this reduced tumor vascularization, tumor areas distant from the underlying stroma exhibited large areas of necrosis (Figure 1, C and D; N) that exhibited typical features in hematoxylin and eosin-stained sections.

Rapid Decrease in Microvessel Density in Tumor-Adjacent Stroma

To study in greater detail the effects of VEGFR-2 inhibition on vascular regression, vessels were quantified in tumor-associated stromal strands identified by immunostaining with antibodies to tenascin-c, a major component of the tumor's stromal ECM.[22] Whereas these intratumoral stromal strands in control transplants were filled with CD31 staining vessels (Figure 2A), a progressive reduction of these vessels was found throughout 4 days after treatment with DC101 (Figure 2; B to D). Of note, these stromal areas, as well as adjacent tumor tissue, were not considered to be necrotic as seen by nuclear staining with Hoechst (Figure 2D).

The differences in tenascin-c-associated vascularization were quantified for all animals and all time points studied. Figure 3 shows a progressive reduction of CD31 staining vessels within the strands of the tumor stroma after treatment with DC101 beginning as soon as 3 hours after treatment. Despite the standard deviations seen in this quantification, statistical significance using the Mann-Whitney test was seen between treated and control animals beginning 24 hours after treatment ($P = 0.03$) and continuing through 48 hours ($P = 0.01$), 72 hours ($P = 0.001$), and 96 hours ($P = 0.01$). In separate experiments analyzing long-term effects of VEGF inhibition, the reduction of CD31 staining within tenascin-c staining areas continued throughout the duration of DC101 treatment. This resulted in a complete lack of vessels within tenascin-c-positive strands of the tumor parenchyma after 8 weeks of DC101 treatment.[21]

Inhibition of VEGFR-2 Reduces Endothelial Cell Proliferation

To better define the effects of VEGFR-2 inhibition on vascular physiology, sections from the same animals were then analyzed for endothelial cell proliferation using immunofluorescent staining with antibodies against BrdU and collagen IV, with staining of all nuclei by Hoechst

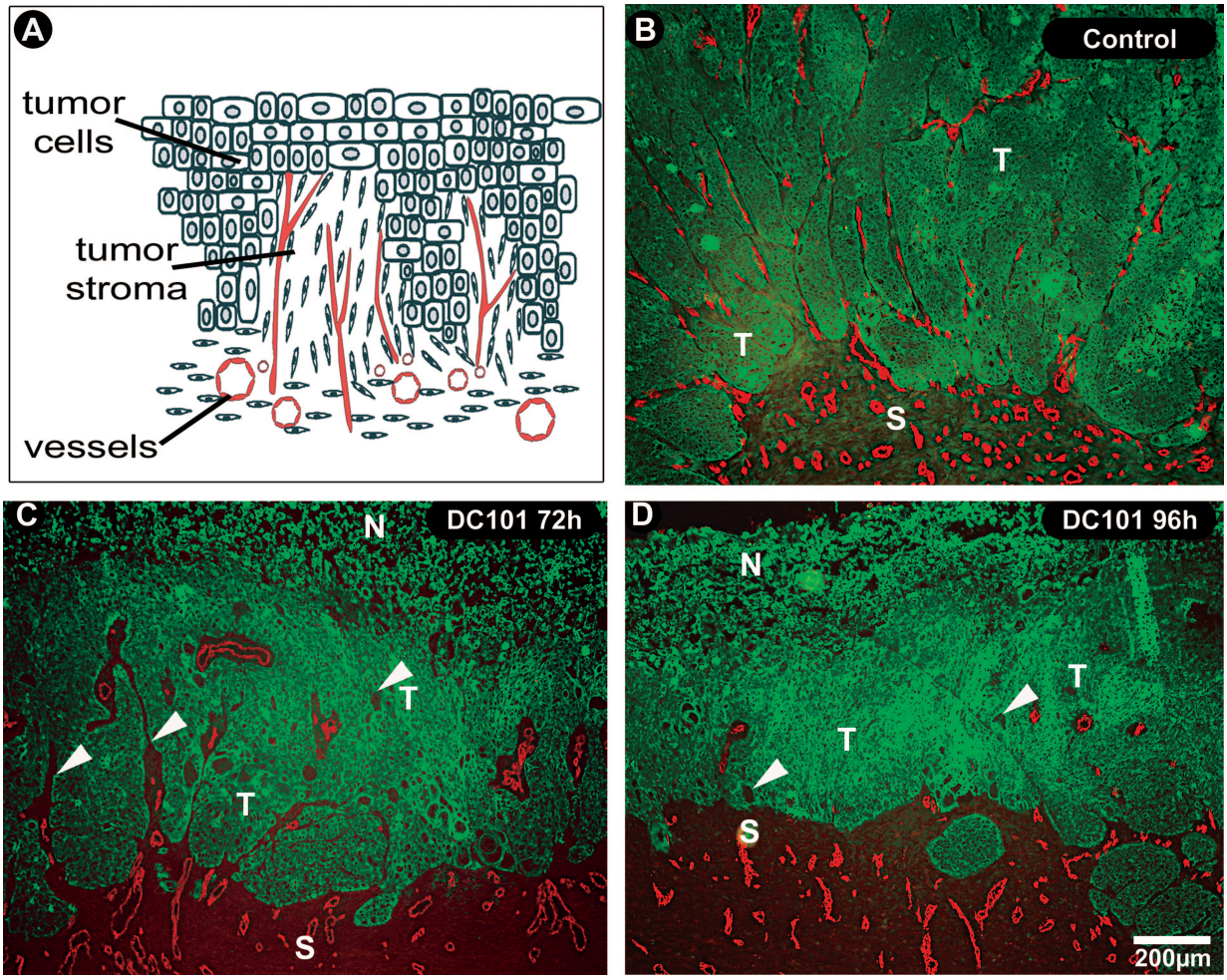

Figure 1. DC101 blocks invasion in surface heterotransplants. **A:** Diagram of surface heterotransplants. Stratified tumor epithelium is invaded by underlying tumor stroma and vessels. **B:** In control A-5RT3 transplants, invasive tumor tissue (T) labeled by a cytokeratin antibody (green) was interspersed with well-vascularized stromal regions (S) with CD31 staining vessels (red). **C** and **D:** Treatment with DC101 blocked vascularization and tumor invasion shown here at 72 hours (**C**) and 96 hours (**D**) after beginning treatment. Both **C** and **D** show a reduction in vital tumor areas (T) with thinning of tumor epithelia under areas of necrosis (N). Furthermore, stromal areas penetrating into the tumor parenchyma showed reduced numbers of CD31 staining vessels (**arrowheads**). Scale bar, 200 μm.

dye. Collagen IV was chosen as a vascular (basement membrane) marker because antibody staining of CD31 was strongly reduced after the acid pretreatment required for unmasking of BrdU incorporated within the DNA. Figure 4 shows representative slides of control (Figure 4A) and 72-hour DC101-treated transplants (Figure 4B) stained for BrdU, collagen IV, and Hoechst. Nuclear Hoechst staining (blue) with overlapping BrdU staining (green) within lumen forming stromal areas positive for collagen IV (red) were considered to be endothelial nuclei undergoing proliferation. Areas, in which reduced vascular density was seen, as described above, were quantified for BrdU expression. This revealed an increasing difference in the percentage of BrdU staining endothelial nuclei between control animals and animals treated by DC101 starting at 3 hours after initial injection and reaching statistical significance after 24 hours ($P < 0.0001$), 48 hours ($P < 0.0001$), 72 hours ($P = 0.01$), and 96 hours ($P = 0.002$) using the Mann-Whitney test (Figure 5). Whereas endothelial proliferation was reduced in those vessels that remained after treatment, no detectable apoptotic endothelial cell could be found at any of the time points studied using the terminal dUTP nick-end labeling (TUNEL) assay (data not shown). This data suggests that VEGFR-2 inhibition is not only capable of limiting the formation of new vessels but may have also caused rapid regression of preformed vessels leading to reduction in microvessel density as soon as 24 hours after initial DC101 treatment and continuing throughout the duration of these studies.

Increase in Normal Vasculature after VEGFR-2 Inhibition

Ultrastructural analysis of the remnant microvasculature within close proximity to tumor cells revealed a rather normal phenotype, as can be seen in representative electron micrographs of tumor-associated vessels. In controls endothelial cells of small vessels closely associated to tumor epithelium (T) were found to be deformed, thinned, and had intercellular gaps (arrowhead), as well as endo-

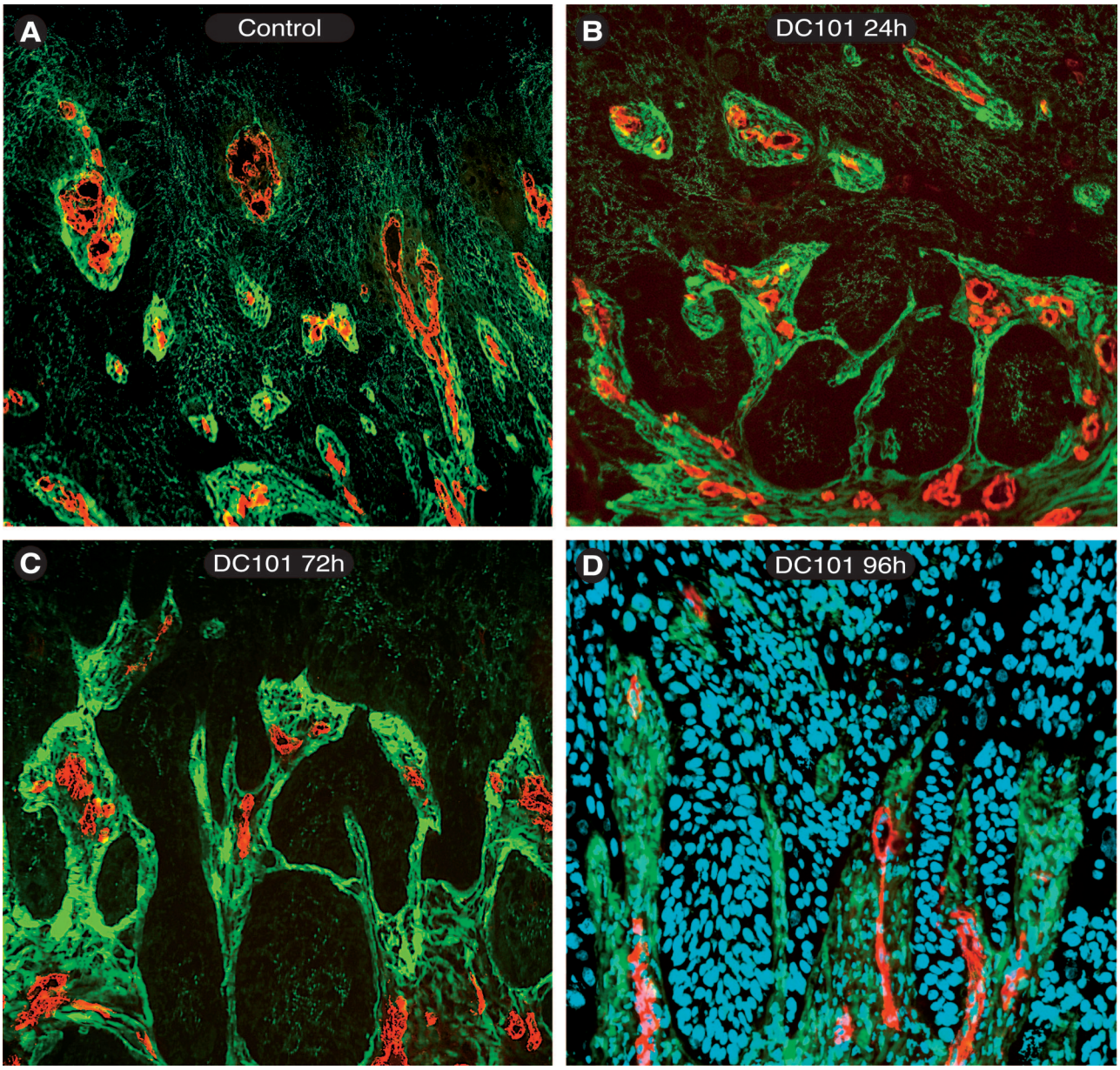

Figure 2. Decrease in microvessel density within intratumoral stromal strands of surface transplants. Fluorescence micrographs showing reduction of CD31 staining vasculature (red) within tumor-associated stromal strands staining for tenascin-c (green) during the duration of VEGFR-2 inhibition by DC101. The four panels compare control transplants to three different DC101 treatment durations. **A:** Control section shows tenascin-c staining stromal strands (green) dispersed throughout tumor tissue (darker green/black) and filled with CD31 staining vessels (red). **B–D:** With increased duration of treatment, there was a progressive reduction in CD31 vessels within tenascin-c staining stroma. **D:** Micrograph with Hoechst nuclear staining (blue), demonstrating that the surrounding tissue is viable and not necrotic after 96 hours of DC101 treatment. **A:** Control; **B:** 24 hours DC101; **C:** 72 hours DC101; and **D:** 96 hours DC101. Original magnifications, ×200.

thelial fenestrations (Figure 6A, box and B; arrowheads). Furthermore, the endothelial basement membrane was almost entirely absent as were associated pericytes. Fibroblasts in a support cell position and extravasated erythrocytes could also been seen in the vicinity of these vessels. Beginning as soon as 24 hours after treatment with DC101, vessels within 100 μm of the tumor showed a rather normal ultrastructural phenotype, which was further increased 96 hours after DC101 treatment (Figure 6, C and D). Endothelial cells displayed normal intercellular junctions (Figure 6C, filled arrowheads) and complete coverage with pericytes (Figure 6, C and D; P). At further magnification, a continuous basement membrane could be seen surrounding both endothelial cells (Figure 6D, filled arrowheads) and endothelial associated pericytes (Figure 6D, outlined arrowheads). These results demonstrate that treatment with DC101 results in a rapid regression of immature vessels leading to the predominance of the mature vascular phenotype.

Re-Established Epithelial Basement Membrane after VEGFR-2 Inhibition

In addition to an increased normalization of the vasculature, a reorganization of the tumor-stromal border zone

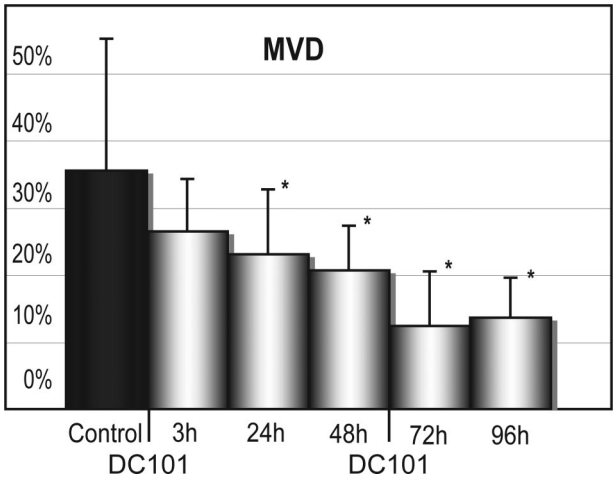

Figure 3. Quantification of microvessel density within intratumoral stromal strands. Quantification of mean vessel density (MVD) within tumor-associated stroma revealed a progressive reduction in CD31 staining vasculature within tenascin-c staining stroma throughout the duration of DC101 treatment. Statistically significant differences (*) were found beginning at 24 hours after initial DC101 treatment. Standard deviations are indicated for each treatment time point by bars. The area of CD31 staining vasculature within tenascin-c staining intratumoral stroma was quantified for all animals studied.

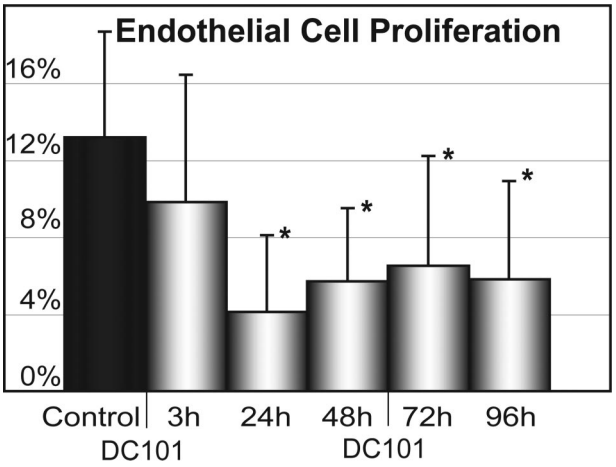

Figure 5. Quantification of endothelial proliferation. Quantification of endothelial proliferation within tumor-associated stroma revealed a progressive reduction in endothelial proliferation throughout the duration of DC101 treatment. Statistically significant differences (*) were found beginning at 24 hours after initial DC101 treatment. Standard deviations are indicated for each treatment time point by bars. Endothelial proliferation within intratumoral strands was quantified for all animals studied.

was also observed. Sections stained for BrdU and collagen IV described above also displayed an increase in collagen IV staining at the epithelial basement membrane zone with duration of DC101 treatment. This staining of the epithelial basement membrane zone was particularly noticeable when sections were counterstained with an antibody to collagen IV and keratin (Figure 7, A and B; arrowheads), with keratin serving as a marker for tumor cells. Whereas in control transplants collagen IV staining was almost exclusively restricted to vessels, the basal pole of the tumor epithelium was increasingly stained after 96 hours of DC101 treatment.

This normalization of the tumor-stromal border was even more obvious in semithin sections and at the ultrastructural level. In semithin sections, the differences in the tumor-stromal border zone between control animals and DC101-treated ones were striking. The tumor-stromal border in untreated control animals (Figure 8A) had an irregular contour with multiple finger-like stromal projections (S) into the overlying tumor epithelium (T) on one side and invading tumor cells on the other. Forty-eight hours after treatment with DC101 (Figure 8B), the tumor-stromal border had a regular contour with a near absence of such finger-like projections and the stromal tissue displayed a reduced number of vessels as compared to

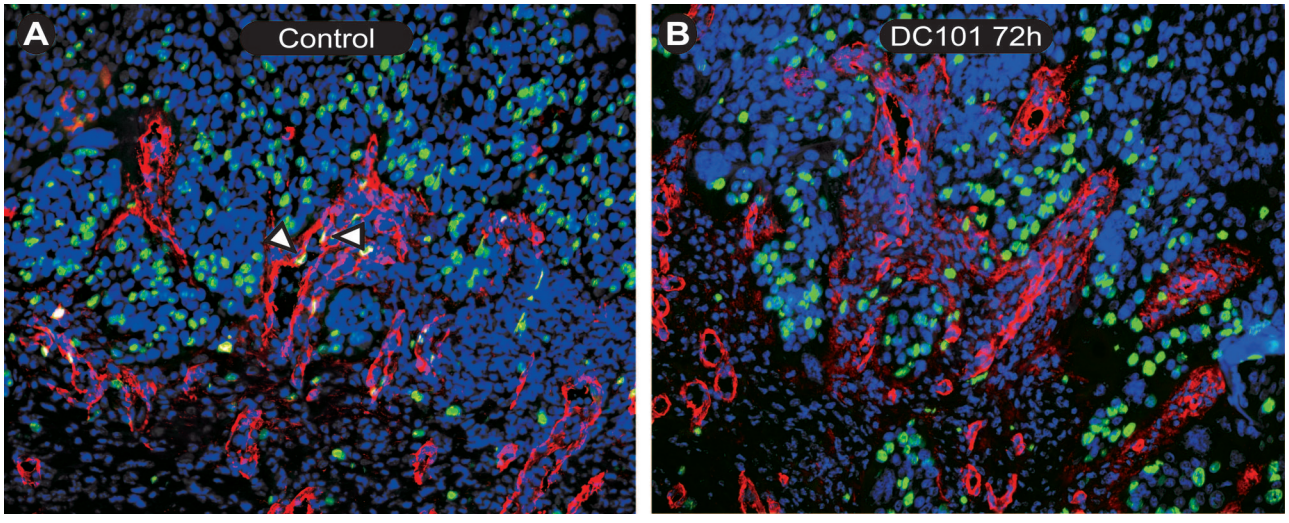

Figure 4. Endothelial proliferation within intratumoral stromal strands. Fluorescence micrographs showing proliferating endothelium within intratumoral stromal strands of control (**A**) and 72-hour DC101-treated (**B**) sections. Triple staining of Hoechst nuclear staining (blue), collagen IV (red), and BrdU (green) revealed tumor areas (predominantly blue staining tumor nuclei) interspersed with collagen IV (red) staining endothelial basement membrane (luminal structures) and tumor epithelial basement membrane (red, stromal-tumor interface). Proliferating nuclei (green) could be seen within both tumor and stromal areas. BrdU staining (green) of collagen IV-positive luminal areas (red) revealed proliferating endothelial cells (**A**, **open arrowheads**). **A:** Control 24 hours; **B:** 72 hours DC101. Original magnifications, ×200.

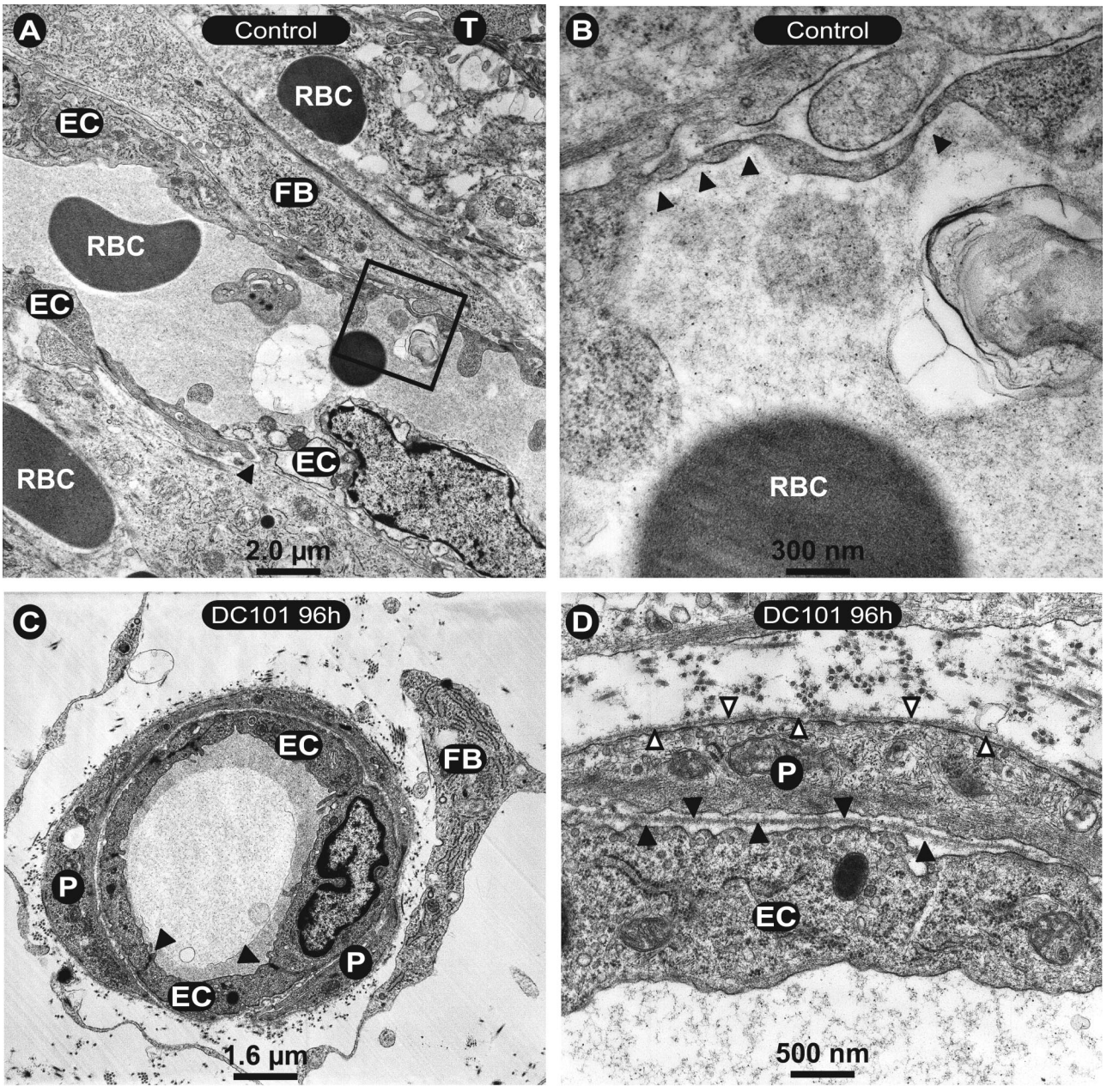

Figure 6. Ultrastructure of tumor microvasculature. **A:** Electron micrographs of control animals show endothelial cells (EC) closely associated to tumor cells (T) and fibroblasts (FB). A predominate endothelial cell nucleus is seen in the **bottom right** endothelial cell. **Arrowhead** indicates a gap between endothelial cells. Extravasated erythrocytes (RBC) are also present. The **box** in **A** is shown at higher magnification in **B** where **arrowheads** highlight endothelial fenestrations. In contrast to control sections, those from DC101-treated animals (**C** and **D**) have a normal phenotype with regular intercellular junctions (**C**, **arrowheads**) and pericytic association (P). At higher magnification (**D**), regular endothelial cell (**D**, **filled arrowheads**) and pericyte (**D**, **open arrowheads**) basement membranes could be detected.

control animals. Significantly, these changes were observed beginning at 24 hours, became more apparent throughout treatment, and were seen in parallel animals at each time point.

The changes toward a normalized epithelial-stromal border zone became striking at the ultrastructural level. In control animals, the irregular tumor-stromal border showed many cellular projections from the tumor into the adjacent stroma (Figure 8C). In contrast, after 96 hours of DC101 treatment, samples from treated animals exhibited a regular tumor cell border adjacent to a stroma rich in collagen bundles (Figure 8, D to F, open arrowhead) separated by long stretches of epithelial basement membrane (Figure 8, E and F, filled arrowheads). Here, a structured basement membrane was formed, including hemidesmosomes with inserted intermediate filaments clearly apparent at higher magnification (Figure 8E, inset). This indicated a normalization of the epithelial-stromal border zone, a characteristic indicator for the reversion of the malignant tumor phenotype to a premalignant one. Remarkably, smoothing of the tumor cell's contour and the appearance of ordered basement membrane

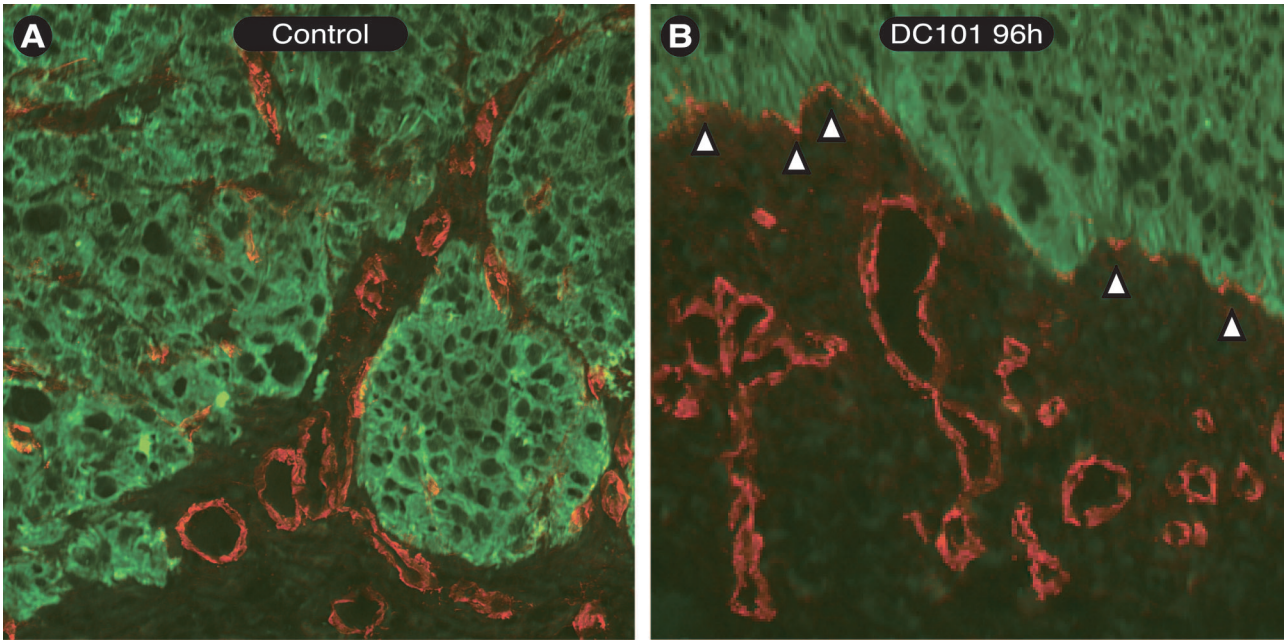

Figure 7. Staining of basement membrane at tumor-stroma border. Immunostaining with antibodies against collagen IV (red) and keratin (green) in control transplants (**A**) showed an irregular tumor-stromal border with stromal projections filled with vasculature (red) between keratin staining tumor cells (green). After 96 hours of DC101 treatment (**B**), staining of collagen IV marked the basal pole of the tumor epithelium (red, **open arrowheads**) and vessels (red luminal structures) away from overlying tumor cells (green). Original magnifications, ×200.

elements also occurred adjacent to remaining thin stromal projections in between tumor epithelium filled with ECM material but devoid of vessels (Figure 8F). The presence of such thin stromal projections at the ultrastructural level suggested that finger-like projections, once devoid of vessels, were either completely abrogated or reduced in size under VEGFR-2 inhibition in large areas of the transplants. Such changes could not be detected in control animals and support our earlier studies in surface transplants showing that long-term VEGFR-2 inhibition is capable of converting the malignant phenotype into a premalignant one.[9,10] This restructuring of stromal elements and normalization of the border zone, suggested altered turnover of ECM components after VEGFR-2 blockade, possibly due to modulated protease expression.

VEGFR-2 Inhibition Abrogates MMP-9 and MMP-13 Expression While Reducing Gelatinase Activity

Matrix-degrading metalloproteases, in particular the gelatinases and interstitial collagenases, have been found to be differentially regulated in premalignant and malignant tumor cells and, importantly, in their adjacent stroma.[24–27] One of the matrix-degrading proteases most frequently associated with malignant tumors is MMP-9 (gelatinase B), which is known to cleave components of the basement membrane.[28] Whereas stromal MMP-9 is only transiently up-regulated in premalignant transplants, this MMP is strongly and persistently expressed in the stroma of malignant transplants.[6,9,10,29] Here it was shown in control surface transplants that MMP-9, visualized by *in situ* hybridization with a mouse-specific probe, was localized in the tumor-associated stroma. Specifically, it was predominately found in the infiltrating stromal strands adjacent to blood vessels, (Figure 9A). Strikingly, this expression was drastically reduced and mostly absent in transplants treated with DC101 for 96 hours (Figure 9B). In malignant control transplants, stromal MMP-9 protein, detected by a mouse-specific antibody, was localized in the tumor-associated stroma, particularly in the infiltration stromal strands mostly adjacent to blood vessels and co-localized with neutrophil granulocytes. On reduction of infiltrating stromal areas in the tumor epithelium of DC101-treated transplants, MMP-9 protein was reduced within the tumor tissue but still present in the underlying tumor-adjacent stroma (data not shown).[21] For murine MMP-13, a mouse interstitial collagenase, a similar localization of RNA expression closely associated with intratumoral vessels was seen in control transplants (Figure 9C). Again short-term treatment with DC101 for 96 hours abolished this expression with exception of a few spots at the tumor-stroma border zone (Figure 9D). This clearly demonstrates rapid and drastic down-regulation of a major gelatinase (MMP-9) and collagenase (MMP-13) in the tumor-stroma border zone after VEGFR-2 blockade by DC101.

However, not only RNA expression was down-regulated. Analysis of protein activity, by EnzChek with DQ-gelatin, showed striking differences in gelatinase activity between control and DC101 transplants. Gelatinase activity in control transplants was restricted to distinct areas in the vicinity to blood vessels at the immediate tumor border and particularly in stromal strands (Figure 10A). After short-term DC101 treatment, this activity was dras-

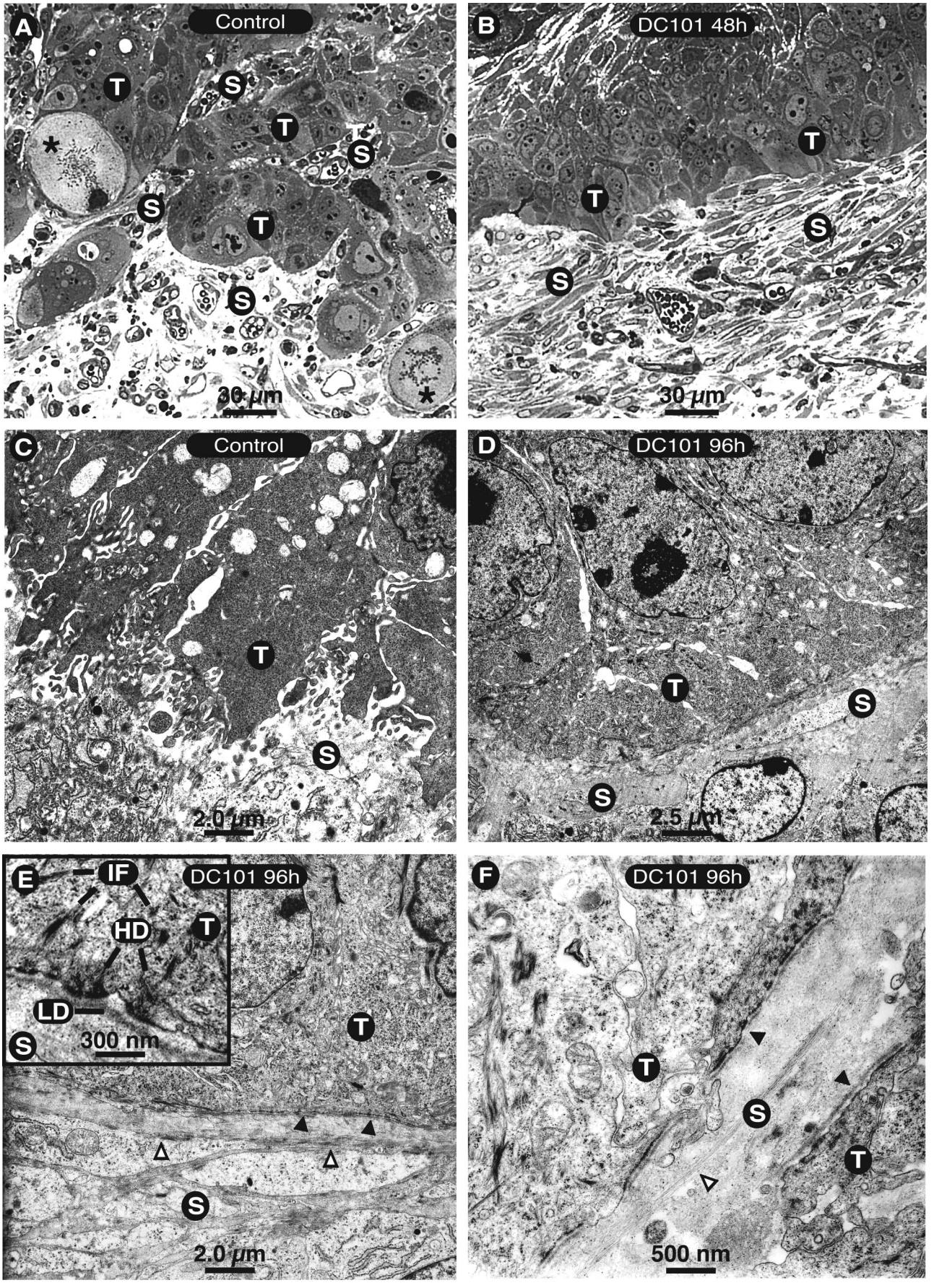
A
Control
T
S
T
S
S
T
S
30 μm
B
DC101 48h
T
T
S
S
30 μm
C
Control
T
S
2.0 μm
D
DC101 96h
T
S
S
2.5 μm
E
IF
HD
T
LD
S
300 nm
DC101 96h
T
S
2.0 μm
F
DC101 96h
T
S
T
500 nm

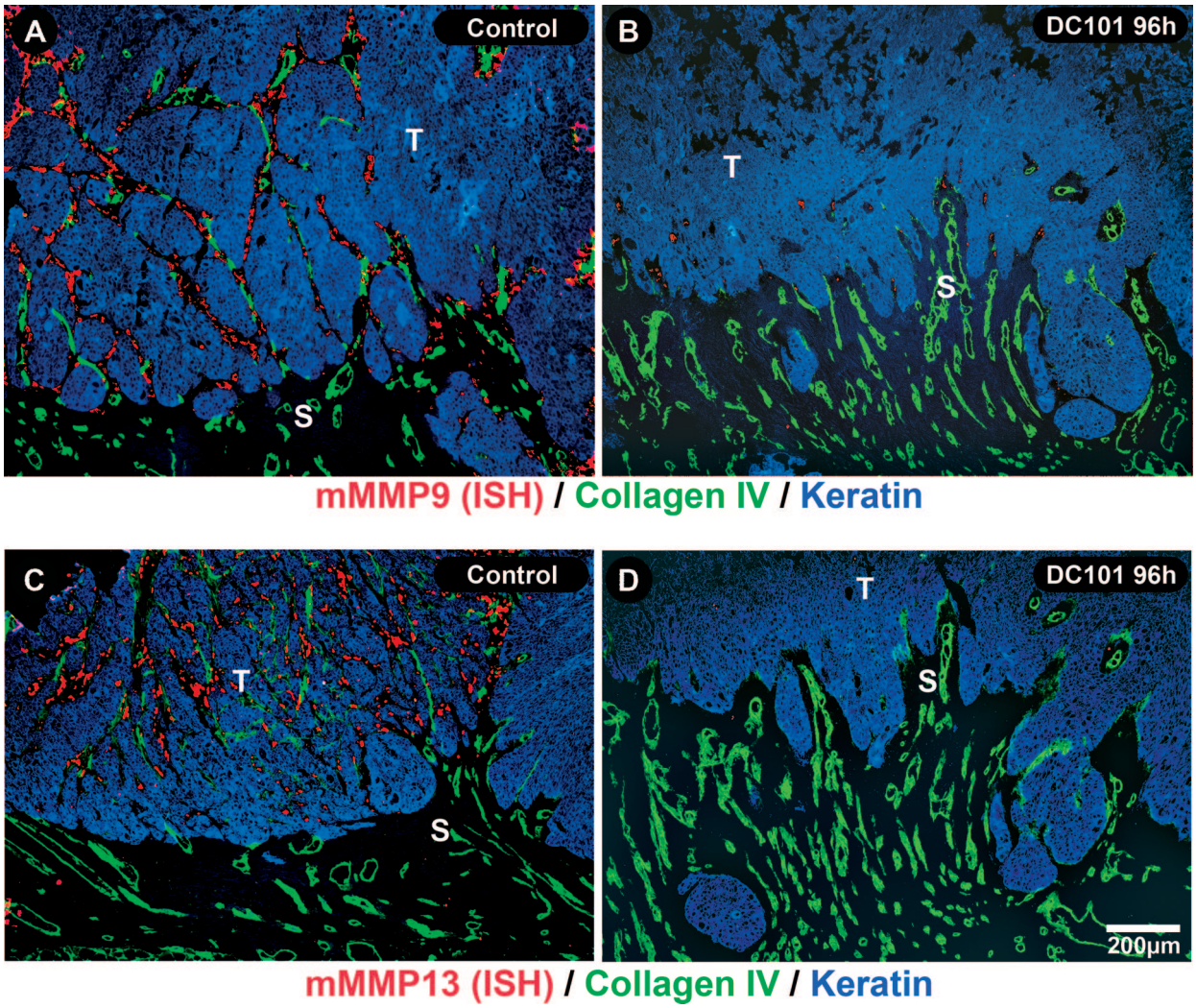

Figure 9. Reduction of MMP-9 and MMP-13 expression 96 hours after DC101. **A–C:** Double-immunofluorescence microscopy staining of tumor cells (T) with a cytokeratin antibody (blue) and endothelial basement membrane by a collagen type IV antibody (green) with nonradioactive *in situ* hybridization signals (red). **A:** Murine MMP-9 expression is localized (ISH, red) in controls to distinct spots in intratumoral stromal strands (S) adjacent to vessels (green) and tumor cells (T) (blue). **B:** After DC101-treatment, there is a reduction of stromal MMP-9 expression to a few spots at the tumor-stromal border. **C:** Murine MMP-13 (red) is strongly expressed in the intratumoral stromal strands close to vessels (green) and to the tumor border (blue). **D:** After short-term treatment with DC101 virtually no expression is seen. Scale bar, 200 μm.

tically reduced to a small rim at the tumor-stroma border (Figure 10B). In brief, the active gelatinase staining area in control transplants was 15.0 ± 8.0%, whereas short-term DC101-treated transplants showed 4.5 ± 2.5% positive gelatinase staining area (Figure 10C). Thus, short-term inhibition of VEGFR-2 signaling caused rapid regression of tumor vasculature with drastically reduced MMP-9 and MMP-13 expression and down-regulated gelatinase activity resulting in a normalized tumor-stromal border zone.

Discussion

This work shows the rapid effects of VEGFR-2 inhibition on vascular regression and reversion of the tumor-phenotype in an experimental model of angiogenesis and tumor invasion using surface heterotransplants of the highly malignant human squamous cell carcinoma cell line A5-RT3. Whereas much evidence exists for the key role of VEGF in angiogenesis,[3,30–32] changes in tumor-stromal morphology resulting from its inhibition have

Figure 8. Ultrastructure of the tumor-stroma border zone. Semithin sections of control (**A**) and 48-hour DC101-treated (**B**) surface transplants. **A:** Control with irregular tumor (T)-stromal (S) borders with mitotic tumor cells (*). Forty-eight hours after DC101 treatment (**B**) there is a regular tumor-stromal border with a reduction of vessels within the underlying stroma as compared to the control (**A**). These changes were pronounced at the ultrastructural level in controls (**C**) with numerous cellular extensions invading the surrounding stroma. **D–F:** After 96 hours of DC101 treatment there is a regular tumor-stromal border with collagen bundles (**open arrowheads**). The treated sample in **E** shows a continuous basement membrane (**filled arrowheads**) along the tumor-stromal border with collagen bundles present in the stroma (**open arrowheads**). The **inset** in **E** shows a higher magnification of the basement membrane after 96 hours of DC101 treatment showing a distinct lamina densa (LD) as well as hemidesmosomes (HD) connected to intermediate filaments (IF). **F:** A 96-hour DC101-treated sample with a finger-like stromal projection with regular tumor-stromal borders, collagen bundles (**open arrowheads**), and an adjacent basement membrane (**filled arrowheads**) between two tumor areas.

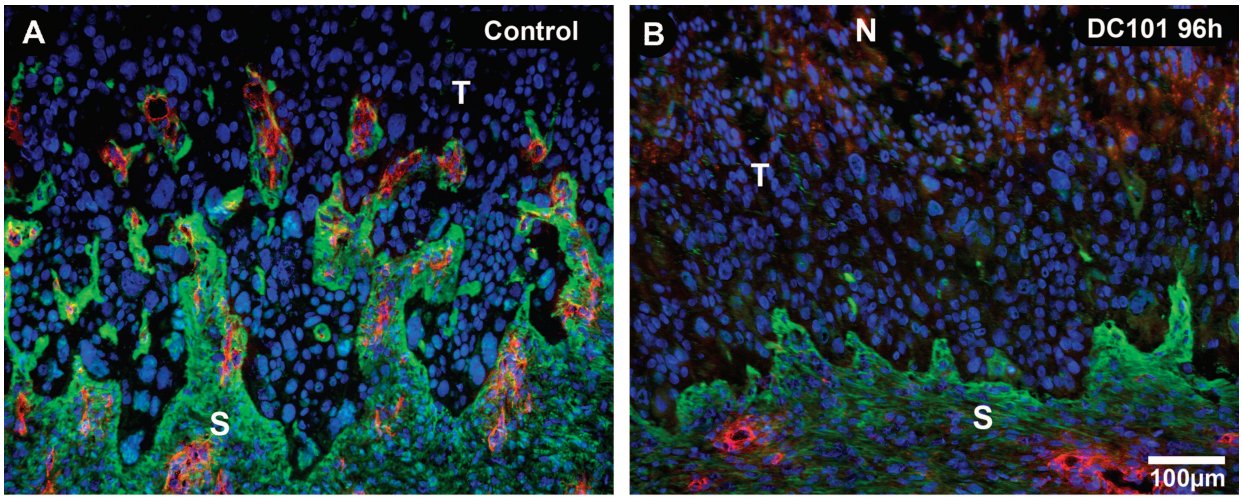

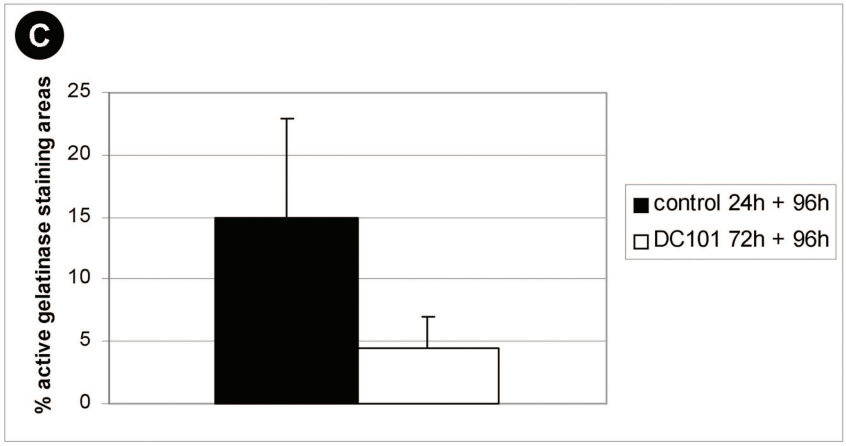

Figure 10. DC101 Inhibits gelatinolytic activity in tumor adjacent stroma. **A** and **B:** *In situ* zymography of gelatinolytic activity (green) with DQ-gelatin as substrate in surface transplants counterstained with an endothelial cell marker (CD31) showing high gelatinase activity in vascularized stroma strands (S) invading the malignant tumor tissue (T) of control transplants (**A**). **B:** After short-term DC101 treatment, gelatinase activity is drastically reduced to a small rim at the tumor-stroma border. **C:** Morphometric quantification of active gelatinase staining. Columns, mean of four to six animals; bars, SD. Scale bar, 100 μm.

been primarily unstudied. Here, the initial phases of a phenotypic shift from a malignant to a premalignant phenotype after VEGFR-2 inhibition were associated with both vascular regression and quiescence and remodeling of the tumor-stromal border. These changes compare to our previous data showing that benign transplants exhibit only transient angiogenesis which rapidly stops on the formation of stratified epithelium.[6,8,9,21] Furthermore, normalization of the tumor-stromal border was detected after DC101 treatment on an ultrastructural level with reduction of tumor cell protrusions from the surrounding stroma and formation of a typical basement membrane at the tumor surface. Additionally, as a consequence of immature vessel regression, DC101 treatment resulted in a normalization of the microvasculature with capillaries exhibiting complete endothelial and pericytic basement membranes and interendothelial junctions as well as close association with surrounding pericytes.

On a histological level, normalization of the tumor-stromal border was characterized by the disappearance of stromal projections from the tumor and reversion of the invasive phenotype. These findings were especially striking at the ultrastructural level, with accumulation of collagen bundles in tumor adjacent stroma and the formation of a well-structured basement membrane attached to the basal tumor cell pole by hemidesmosomes. This was striking considering the aggressive growth characteristics of the squamous cell carcinoma cell line A5-RT3.[20] Formation of a structured basement membrane is a diagnostic feature of benign or premalignant tumors. Additionally, there has been an inverse correlation reported between the amount of tumor-associated basement membrane and tumor aggressiveness.[33] Therefore, the normalization of the basement membrane shown here is a clear indication of a phenotypic shift in the invasive malignant transplants to a premalignant tumor phenotype after VEGFR-2 inhibition.

The extent to which basement membrane and stromal maturation are due to altered expression of ECM components and/or their reduced turnover through lowered protease activity remains to be studied.[34] However, our data showing reduced expression of both MMP-9 (gelatinase B) and MMP-13 (collagenase), with reduced levels of gelatinase activity as seen by *in situ* zymography indicated that altered protease expression may play an important role in the maturation process. MMP-9 is one of the matrix-degrading proteases most frequently associ-

ated with malignant tumors and is known to cleave components of the ECM, particularly those of the basement membrane.[28,35] It has been shown to facilitate endothelial cell migration as well as tumor cell invasion.[36,37] Furthermore, MMP-9-deficient mice display inhibited angiogenesis, tumor progression, and metastasis.[26,27,38] Our studies not only showed a reduction in the expression of MMP-9 after VEGFR-2 inhibition but also a reduction in general gelatinase activity, which suggested their inhibition plays a crucial role in the stromal maturation process after DC101 treatment. Comparably, reduced MMP-13 expression in tumor-adjacent stroma most likely contributed to decreased turnover of collagen type I. Additionally, blockade of VEGFR-2 by a tyrosine kinase inhibitor also reduces the secretion of other matrix metalloproteases such as MMP-2 and MMP-3 in endothelial cells, inhibiting their migration.[39] However, the molecular mechanisms by which MMPs promote tumor invasion and angiogenesis are still poorly understood.[40] We hypothesize that reduced expression of MMP-9 and MMP-13, with subsequently reduced gelatinase activity was responsible for reduced degradation of basement membrane components, therefore allowing for their accumulation and structural reorganization. In particular, laminin is a critical determinant of morphogenesis and differentiation and directs tissue-specific gene expression in tissue-type *in vitro* models.[41] Its reduced turnover due to MMP-9 down-regulation may contribute not only to basement membrane reconstitution but also to normalization of epithelial polarity and, thus, to the reverted tumor phenotype. Significantly, these normalization effects were not caused by the direct blockade of VEGF on tumor cells. The human A-5RT3 tumor cells express VEGFR-2 *in vitro* at the RNA level (data not shown), however, the mouse-specific DC101 antibody does not cross-react with the human VEGFR-2.[19] Thus, the normalizing effect on the tumor cell phenotype must be caused indirectly by stromal alterations.[42–44] Although the MMP-9 and MMP-13 synthesizing cell types have not yet been identified, the localization of RNA signals indicated that perivascular cells, most probably fibroblasts, were likely candidates. Their localization close to endothelial cells and tumor cells suggests that their expression was induced by paracrine signals from both neighboring cells. Blockade of endothelial cell activation resulted in down-regulation of both MMPs, suggesting a major paracrine role of endothelial cell-derived factors to control these stromal MMPs.

Because these stromal alterations were seen after alteration of VEGF signaling by DC101 it can be assumed that endothelial cell activity may have essential functional consequences for the pathophysiology of the tumor stroma. Although features of stromal maturation and tumor phenotype reversion are also seen in subcutaneous tumors, they are particularly well demonstrated in the surface transplants used here with their distinct geometry and the well-defined stromal development.[9] In this *in vivo* model, early changes in the tumor-stroma border are manifest and available for detailed analysis. As with other *in vivo* models, quantification of results is still difficult and remains restricted to morphometric analysis of vascularization by determining mean vessel density[31,45,46] or by counting nuclei with incorporated BrdU as mean of cell proliferation.

In addition to the ultrastructural changes seen at the tumor-stromal border zone, use of the surface transplant model displayed significant changes at the vascular level. These changes began as soon as 24 hours after DC101 treatment, progressing throughout the latest time points studied. Treatment resulted in a significant reduction of endothelial fenestrations (considered to be induced by VEGF[47]) and a normalization of interendothelial junctions. After treatment, the relation of pericyte-free microvasculature shifted toward vessels associated with pericytes with normalization of both endothelial and pericytic basement membranes. These changes coincided with the reduction of vessels from stromal projections as shown by simultaneous staining of CD31 and tenascin-c, a major component of the tumor-stromal ECM.[22,48,49] This latter effect was apparently due to the elimination of VEGF signaling as a critical survival factor for endothelial cells of immature vessels.[17] This resulted in a relative increase in mature vessels and was probably not a direct normalizing effect of DC101. Interestingly, quantification of vascular regression showed a stepwise reduction in the number of CD31 staining vessels within tenascin-c staining ECM until the latest time point measured. Furthermore, separate studies under long-term DC101 treatment showed a nearly complete absence of CD31 staining vessels from such areas.[21] This suggested that such vascular regression is sustained throughout the course of VEGFR-2 inhibition, indicating the continuing need of VEGF as an endothelial survival factor for the tumor microvasculature. Notably, the time course of vascular regression found in this study also mirrored the decrease in tumor vasculature previously documented by MRI imaging studies of heterotransplants.[49]

Furthermore, studies in other model systems also support the findings on vascular regression reported here. Brown and colleagues[50] have demonstrated that vascular pruning of immature tumor vessels may occur as soon as 24 hours after treatment with VEGFR-2 inhibitors, resulting in normalization of tumor vasculature. Additionally, recent studies indicate that inhibition of VEGFR-1 and R-2 by VEGF-Trap, or inhibition of multiple angiogenic compounds by the tyrosine kinase inhibitor AG013736, result in a reduction of vascularity, vascular perfusion, and VEGFR-2 expression between 1 and 7 days after treatment.[51] The changes in ECM morphology and MMP-9 and MMP-13 expression shown here, therefore, demonstrate a normalization of tumor phenotype concomitant with that of the tumor vasculature after VEGFR-2 inhibition.

The exact mechanism of vascular regression through VEGFR-2 inhibition was, however, only partly elucidated in our studies. Whereas endothelial proliferation was reduced in those vessels that remained after treatment, no detectable apoptotic endothelial cells could be found using the TUNEL assay at any of the time points (beginning 3 hours after initial treatment) studied here (data not shown). This suggests that endothelial apoptotic processes associated with VEGF inhibition may be difficult to detect due to the short time frame in which they can be

ascertained by standard TUNEL assays after inhibition of VEGFR-2. The extent to which vascular maturity altered responses to VEGF inhibition was not directly considered in this study. In separate studies using the same assay, the number of vessels associated with pericyte markers considered to reflect vascular maturity, such as α-smooth muscle actin, was only found to increase after treatment periods of up to 2 weeks in animals receiving multiple treatments.[21]

Also important in vascular regression, the role of the angiopoietins in this model system has yet to be evaluated. The recent increase in understanding of the angiopoietins and their receptor tie-2 suggest that, in the absence of VEGF, angiopoietin 2 (ang-2) may be the causal factor in vascular regression and apoptosis.[52–54] Elegantly demonstrated by Lobov and colleagues using the pupillary membrane assay of the murine eye, ang-2 has been reported to be proapoptotic and enhance vascular regression in the absence of VEGF.[52] The study of the early stages of vascular regression reported on here, in the context of tumor-associated stroma stained by tenascin-c, provide a unique platform for the study of vascular regression and studies are planned to assess the role of the angiopoietins using this model system.

This study demonstrates the rapid effects of VEGFR-2 inhibition on reduction in vascular density, protease expression, and modulation of tumor-stromal morphology. The decreased expression of a major gelatinase represented by MMP-9 and an interstitial collagenase (MMP-13) as well as the regression of preformed vessels after treatment with DC101 was thought to aid in the reversion of the tumor phenotype from a malignant to a premalignant one beginning as soon as 24 hours after treatment. Further studies into the detailed mechanisms of VEGF inhibition on MMP-9 and MMP-13 expression and its consequences on the tumor-stroma phenotype are currently underway.

References

1. Folkman J: Angiogenesis in cancer, vascular, rheumatoid and other disease. Nat Med 1995, 1:27–31
2. Jain RK, Carmeliet PF: Vessels of death or life. Sci Am 2001, 285:38–45
3. Ferrara N: VEGF and the quest for tumour angiogenesis factors. Nat Rev Cancer 2002, 2:795–803
4. Alitalo K, Carmeliet P: Molecular mechanisms of lymphangiogenesis in health and disease. Cancer Cell 2002, 1:219–227
5. Fusenig NE, Skobe M, Vosseler S, Hansen M, Lederle W, Airola K, Tomakidi P, Stark HJ, Steinbauer H, Mirancea N, Boukamp P, Breitkreutz D: Tissue models to study tumor-stroma interactions. Proteases and Their Inhibitors in Cancer Metastasis. Edited by Muschel RJFJ. Dordrecht, Kluwer Academic Publishers, 2002, pp 205–223
6. Mueller MM, Fusenig NE: Friends or foes—bipolar effects of the tumour stroma in cancer. Nat Rev Cancer 2004, 4:839–849
7. Fusenig NE, Boukamp P: Multiple stages and genetic alterations in immortalization, malignant transformation, and tumor progression of human skin keratinocytes. Mol Carcinog 1998, 23:144–158
8. Skobe M, Rockwell P, Goldstein N, Vosseler S, Fusenig NE: Halting angiogenesis suppresses carcinoma cell invasion. Nat Med 1997, 3:1222–1227
9. Mueller MM, Fusenig NE: Tumor-stroma interactions directing phenotype and progression of epithelial skin tumor cells. Differentiation 2002, 70:486–497
10. Boukamp P, Petrussevska RT, Breitkreutz D, Hornung J, Markham A, Fusenig NE: Normal keratinization in a spontaneously immortalized aneuploid human keratinocyte cell line. J Cell Biol 1988, 106:761–771
11. Boukamp P, Stanbridge EJ, Foo DY, Cerutti PA, Fusenig NE: c-Ha-ras oncogene expression in immortalized human keratinocytes (HaCaT) alters growth potential in vivo but lacks correlation with malignancy. Cancer Res 1990, 50:2840–2847
12. Bajou K, Noel A, Gerard RD, Masson V, Brunner N, Holst-Hansen C, Skobe M, Fusenig NE, Carmeliet P, Collen D, Foidart JM: Absence of host plasminogen activator inhibitor 1 prevents cancer invasion and vascularization. Nat Med 1998, 4:923–928
13. Bajou K, Masson V, Gerard RD, Schmitt PM, Albert V, Praus M, Lund LR, Frandsen TL, Brunner N, Dano K, Fusenig NE, Weidle U, Carmeliet G, Loskutoff D, Collen D, Carmeliet P, Foidart JM, Noel A: The plasminogen activator inhibitor PAI-1 controls in vivo tumor vascularization by interaction with proteases, not vitronectin. Implications for antiangiogenic strategies. J Cell Biol 2001, 152:777–784
14. Skobe M, Fusenig NE: Tumorigenic conversion of immortal human keratinocytes through stromal cell activation. Proc Natl Acad Sci USA 1998, 95:1050–1055
15. Bleuel K, Popp S, Fusenig NE, Stanbridge EJ, Boukamp P: Tumor suppression in human skin carcinoma cells by chromosome 15 transfer or thrombospondin-1 overexpression through halted tumor vascularization. Proc Natl Acad Sci USA 1999, 96:2065–2070
16. Javaherian A, Vaccariello M, Fusenig NE, Garlick JA: Normal keratinocytes suppress early stages of neoplastic progression in stratified epithelium. Cancer Res 1998, 58:2200–2208
17. Benjamin LE, Golijanin D, Itin A, Pode D, Keshet E: Selective ablation of immature blood vessels in established human tumors follows vascular endothelial growth factor withdrawal. J Clin Invest 1999, 103:159–165
18. Carmeliet P: Mechanisms of angiogenesis and arteriogenesis. Nat Med 2000, 6:389–395
19. Witte L, Hicklin DJ, Zhu Z, Pytowski B, Kotanides H, Rockwell P, Bohlen P: Monoclonal antibodies targeting the VEGF receptor-2 (Flk1/KDR) as an anti-angiogenic therapeutic strategy. Cancer Metastasis Rev 1998, 17:155–161
20. Mueller MM, Peter W, Mappes M, Huelsen A, Steinbauer H, Boukamp P, Vaccariello M, Garlick J, Fusenig NE: Tumor progression of skin carcinoma cells in vivo promoted by clonal selection, mutagenesis, and autocrine growth regulation by granulocyte colony-stimulating factor and granulocyte-macrophage colony-stimulating factor. Am J Pathol 2001, 159:1567–1579
21. Vosseler S, Mirancea N, Bohlen P, Mueller MM, Fusenig NE: Angiogenesis inhibition by VEGFR-2 blockade reduces stromal MMP expression, normalizes stromal tissue and reverts tumor phenotype. Cancer Res 2005, 65:1294–1305
22. Chiquet-Ehrismann R, Chiquet M: Tenascins: regulation and putative functions during pathological stress. J Pathol 2003, 200:488–499
23. Moorman AF, De Boer PA, Vermeulen JL, Lamers WH: Practical aspects of radio-isotopic in situ hybridization on RNA. Histochem J 1993, 25:251–266
24. Borchers AH, Steinbauer H, Schafer BS, Kramer M, Bowden GT, Fusenig NE: Fibroblast-directed expression and localization of 92-kDa type IV collagenase along the tumor-stroma interface in an in vitro three-dimensional model of human squamous cell carcinoma. Mol Carcinog 1997, 19:258–266
25. Airola K, Fusenig NE: Differential stromal regulation of MMP-1 expression in benign and malignant keratinocytes. J Invest Dermatol 2001, 116:85–92
26. Werb Z, Vu TH, Rinkenberger JL, Coussens LM: Matrix-degrading proteases and angiogenesis during development and tumor formation. APMIS 1999, 107:11–18
27. Coussens LM, Tinkle CL, Hanahan D, Werb Z: MMP-9 supplied by bone marrow-derived cells contributes to skin carcinogenesis. Cell 2000, 103:481–490
28. Huang S, Van Arsdall M, Tedjarati S, McCarty M, Wu W, Langley R, Fidler IJ: Contributions of stromal metalloproteinase-9 to angiogenesis and growth of human ovarian carcinoma in mice. J Natl Cancer Inst 2002, 94:1134–1142
29. Masson V, de la Ballina LR, Munaut C, Wielockx B, Jost M, Maillard C, Blacher S, Bajou K, Itoh T, Itohara S, Werb Z, Libert C, Foidart JM, Noel A: Contribution of host MMP-2 and MMP-9 to promote tumor

vascularization and invasion of malignant keratinocytes. FASEB J 2005, 19:234–236
30. Dvorak HF, Brown LF, Detmar M, Dvorak AM: Vascular permeability factor/vascular endothelial growth factor, microvascular hyperpermeability, and angiogenesis. Am J Pathol 1995, 146:1029–1039
31. Klement G, Baruchel S, Rak J, Man S, Clark K, Hicklin DJ, Bohlen P, Kerbel RS: Continuous low-dose therapy with vinblastine and VEGF receptor-2 antibody induces sustained tumor regression without overt toxicity. J Clin Invest 2000, 105:R15–R24
32. Prewett M, Huber J, Li Y, Santiago A, O'Connor W, King K, Overholser J, Hooper A, Pytowski B, Witte L, Bohlen P, Hicklin DJ: Antivascular endothelial growth factor receptor (fetal liver kinase 1) monoclonal antibody inhibits tumor angiogenesis and growth of several mouse and human tumors. Cancer Res 1999, 59:5209–5218
33. Barsky SH, Siegal GP, Jannotta F, Liotta LA: Loss of basement membrane components by invasive tumors but not by their benign counterparts. Lab Invest 1983, 49:140–147
34. Hagedorn HG, Bachmeier BE, Nerlich AG: Synthesis and degradation of basement membranes and extracellular matrix and their regulation by TGF-beta in invasive carcinomas. Int J Oncol 2001, 18:669–681
35. Yu Q, Stamenkovic I: Cell surface-localized matrix metalloproteinase-9 proteolytically activates TGF-beta and promotes tumor invasion and angiogenesis. Genes Dev 2000, 14:163–176
36. Nelson AR, Fingleton B, Rothenberg ML, Matrisian LM: Matrix metalloproteinases: biologic activity and clinical implications. J Clin Oncol 2000, 18:1135–1149
37. Stetler-Stevenson WG: Matrix metalloproteinases in angiogenesis: a moving target for therapeutic intervention. J Clin Invest 1999, 103:1237–1241
38. Itoh T, Tanioka M, Matsuda H, Nishimoto H, Yoshioka T, Suzuki R, Uehira M: Experimental metastasis is suppressed in MMP-9-deficient mice. Clin Exp Metastasis 1999, 17:177–181
39. Wagner S, Fueller T, Hummel V, Rieckmann P, Tonn JC: Influence of VEGF-R2 inhibition on MMP secretion and motility of microvascular human cerebral endothelial cells (HCEC). J Neurooncol 2003, 62:221–231
40. Quaranta V: Cell migration through extracellular matrix: membrane-type metalloproteinases make the way. J Cell Biol 2000, 149:1167–1170
41. Streuli CH, Schmidhauser C, Bailey N, Yurchenco P, Skubitz AP, Roskelley C, Bissell MJ: Laminin mediates tissue-specific gene expression in mammary epithelia. J Cell Biol 1995, 129:591–603
42. Olumi AF, Grossfeld GD, Hayward SW, Carroll PR, Tlsty TD, Cunha GR: Carcinoma-associated fibroblasts direct tumor progression of initiated human prostatic epithelium. Cancer Res 1999, 59:5002–5011
43. Bissell MJ, Radisky DC, Rizki A, Weaver VM, Petersen OW: The organizing principle: microenvironmental influences in the normal and malignant breast. Differentiation 2002, 70:537–546
44. Tlsty TD: Stromal cells can contribute oncogenic signals. Semin Cancer Biol 2001, 11:97–104
45. Carmeliet P, Jain RK: Angiogenesis in cancer and other diseases. Nature 2000, 407:249–257
46. Kim ES, Serur A, Huang J, Manley CA, McCrudden KW, Frischer JS, Soffer SZ, Ring L, New T, Zabski S, Rudge JS, Holash J, Yancopoulos GD, Kandel JJ, Yamashiro DJ: Potent VEGF blockade causes regression of coopted vessels in a model of neuroblastoma. Proc Natl Acad Sci USA 2002, 99:11399–11404
47. Feng D, Nagy JA, Hipp J, Dvorak HF, Dvorak AM: Vesiculo-vacuolar organelles and the regulation of venule permeability to macromolecules by vascular permeability factor, histamine, and serotonin. J Exp Med 1996, 183:1981–1986
48. Jones FS, Jones PL: The tenascin family of ECM glycoproteins: structure, function, and regulation during embryonic development and tissue remodeling. Dev Dyn 2000, 218:235–259
49. Kiessling F, Farhan N, Lichy MP, Vosseler S, Heilmann M, Krix M, Bohlen P, Miller DW, Mueller MM, Semmler W, Fusenig NE, Delorme S: Dynamic contrast-enhanced magnetic resonance imaging rapidly indicates vessel regression in human squamous cell carcinomas grown in nude mice caused by VEGF receptor 2 blockade with DC101. Neoplasia 2004, 6:213–223
50. Brown EB, Campbell RB, Tsuzuki Y, Xu L, Carmeliet P, Fukumura D, Jain RK: In vivo measurement of gene expression, angiogenesis and physiological function in tumors using multiphoton laser scanning microscopy. Nat Med 2001, 7:864–868
51. Inai T, Mancuso M, Hashizume H, Baffert F, Haskell A, Baluk P, Hu-Lowe DD, Shalinsky DR, Thurston G, Yancopoulos GD, McDonald DM: Inhibition of vascular endothelial growth factor (VEGF) signaling in cancer causes loss of endothelial fenestrations, regression of tumor vessels, and appearance of basement membrane ghosts. Am J Pathol 2004, 165:35–52
52. Lobov IB, Brooks PC, Lang RA: Angiopoietin-2 displays VEGF-dependent modulation of capillary structure and endothelial cell survival in vivo. Proc Natl Acad Sci USA 2002, 99:11205–11210
53. Holash J, Maisonpierre PC, Compton D, Boland P, Alexander CR, Zagzag D, Yancopoulos GD, Wiegand SJ: Vessel cooption, regression, and growth in tumors mediated by angiopoietins and VEGF. Science 1999, 284:1994–1998
54. Ramsauer M, D'Amore PA: Getting Tie(2)d up in angiogenesis. J Clin Invest 2002, 110:1615–1617